GEOGRAFICKÝ ČASOPIS / GEOGRAPHICAL JOURNAL 77 (2025) 4, 183-199
DOI: https://doi.org/10.31577/geogrcas.2025.77.4.02

INSTITUTE OF GEOGRAPHY SLOVAK ACADEMY OF SCIENCES

Geografický časopis
Geographical Journal

A detection of channel bathymetry from drones: accuracy of point clouds and RGB images for reconstruction of channel-bed topography

Miloš Rusnák[1*], Rohit Sharma[2], Valentín Sočuvka[3], Ashraf MD[1,6], Tomáš Goga[1], Ján Kaňuk[4], Lukáš Michaleje[1], Hamid Afzali[1,6], Ján Sládek[1], Ján Šašak[5], Zulfequar Ahmad[2], Dev Garg Rahul[2]

[1] Institute of Geography, Slovak Academy of Sciences, Bratislava, Slovakia, geogmilo@savba.sk, tomas.goga@savba.sk, ashraf.md@savba.sk, geoglumi@savba.sk, hamid.afzali@savba.sk, geogslad@savba.sk
[2] Indian Institute of Technology Roorkee, India, r_sharma@ce.iitr.ac.in, z.ahmad@ce.iitr.ac.in, rdgarg@ce.iitr.ac.in
[3] Institute of Hydrology, Slovak Academy of Sciences, Bratislava, Slovakia, socuvka@uh.savba.sk
[4] PHOTOMAP, s.r.o., Košice, Slovakia, jan.kanuk@photomap.sk
[5] Institute of Geography, Faculty of Science, Pavol Jozef Šafárik University in Košice, Košice, Slovakia, jan.sasak@upjs.sk
[6] Department of Physical Geography and Geoecology Faculty, Comenius University, Bratislava, Slovakia
* Corresponding author

Abstract

Channel bathymetry detection focuses on extracting riverbed topography, and it is a primary tool for analysing channel dynamics, sedimentary processes, and habitat structures. A key challenge in underwater bathymetry is accurately capturing high-resolution topography of the channel bed. Knowledge of underwater channel shape and topography is a fundamental parameter essential for hydraulic modelling, monitoring of channel bed changes, and environmental assessments of riparian ecosystems, including underwater vegetation, grain size, and fish habitats. The objective of this study is to reconstruct the channel topography of the shallow, multi-channel braided Belá River and the artificial Gabčíkovo-Topoľníky canal, featuring shallower and deeper sections, to critically evaluate the efficiency of various UAV-based bathymetric methods. Riverbed topography was reconstructed by two main approaches: through-water photogrammetry and spectral depth estimation. Results were validated through a traditional field survey, which included field measurements and a sonar survey. The accuracy of bathymetry refraction correction achieved a mean error of less than 1 cm, and the root mean square error (RMSE) reached a maximum of 13 cm for the Belá River site, as validated by field depth measurements. The artificial canal Gabčíkovo-Topoľníky exhibited errors (RMSE) ranging from 12 to 30 cm, as validated by sonar. The optical bathymetry approach pointed to errors ranging from 14.7 to 23.3 cm with a regression model R^2 from 0.47 to 0.53.

Key words:
bathymetry, point cloud, Unmanned Aerial Vehicle, UAV, RGB images, water depth, refraction, spectral modelling

1 INTRODUCTION

Bathymetry is defined as a method that enables the identification of underwater topography and plays a critical role in environmental and geomorphological research by providing detailed measurements of riverbed morphology. Understanding underwater topography is essential for various applications, including hydrology, sediment transport studies, flood modelling, and aquatic ecosystem management (Woodget et al., 2017). River bathymetry focuses on mapping riverbeds to analyse channel dynamics, sedimentary processes, and habitat structures, which are vital for both scientific inquiry and practical applications such as navigation, water resource management, and climate change adaptation.

The study of bathymetry has evolved significantly from rudimentary depth-sounding techniques to advanced remote sensing technologies. Early bathymetric measurements date back to the 19th century, when sailors used weighted lines to measure water depths (Lurton, 2010). The development of echo sounding in the early 20th century revolutionised bathymetric mapping by enabling continuous depth recordings. Advances in the late 20th and 21st centuries introduced traditional profiling or cross-section measurement, sonar, green LiDAR (utilising a 532 nm green wavelength), and remote sensing-derived bathymetry, drastically improving accuracy, efficiency, and ecological applications (Smith & Sandwell, 1997). Despite the advancement in bathymetric technologies, several limitations and challenges persist. Environmental factors, such as water turbidity, can significantly impact the accuracy and efficiency of bathymetry surveys using optical, LiDAR, or sonar methods (Lague & Feldmann, 2020; Smith & Sandwell, 1997).

Among the most promising innovations in shallow bathymetry is the deployment of unmanned aerial vehicles (UAVs), which provide a cost-effective, adaptable, and scalable means of capturing high-resolution bathymetric data. UAVs equipped with RGB cameras facilitate novel methodologies such as Structure-from-Motion (SfM) photogrammetry, which

reconstructs topography through multi-view stereo detection (Woodget et al., 2018). Submerged topography from UAV is detected by two main approaches: i) topography detected using the spectral-depth approach (optical bathymetry) based on the statistical correlations between spectral band properties and empirical data; ii) light refraction correction in through-water photogrammetry, that use SfM-photogrammetry to reconstruct channel topography with application of elevation correction, which is caused by bending of light rays as they pass from air to water boundary (see examples and detailed information about river submerged topography detection in Tab. 1).

Optically derived bathymetry presents an approach to mapping underwater topography by exploiting the differential absorption and scattering properties of water across multiple spectral bands. This method has demonstrated high precision in clear-water environments, with studies confirming a strong correlation between spectral properties and in situ depth measurements (Lyzenga, 1978; Legleiter, 2021; Legleiter & Roberts, 2005). However, the effectiveness is significantly influenced by environmental conditions such as turbidity, substrate reflectance, and light penetration depth (Yunus et al., 2019).

Direct topography mapping of submerged channels from UAVs requires refraction correction based on the elevation of the water's edge (Woodget et al., 2017, 2019; Woodget & Austrums, 2017) or the use of a multi-angle refraction correction (Dietrich, 2017). This technique has gained widespread attention due to its ability to generate high-density point clouds and digital elevation models (DEMs) with sub-centimetre accuracy (Woodget et al., 2017). However, the primary challenge in through-water photogrammetry remains the optical distortion caused by refraction, which alters the perceived depth of submerged features. To address this issue, researchers have developed correction algorithms that incorporate site-specific refraction indices and water surface modelling (Woodget et al., 2019).

This study aims to critically evaluate the efficiency of various UAV-based bathymetric methods, comparing through-water photogrammetry, spectral depth estimation, and traditional field surveys by systematically applying UAV-derived bathymetry in shallow, fluvial environments. Ultimately, this work contributes to the ongoing advancement of high-resolution topographic and bathymetric mapping techniques, addressing key challenges in fluvial geomorphology and hydrology. The main task is related to: i) the evaluation of refraction-correction SfM approach for bathymetry detection; ii) the evaluation of optical approach; iii) differences between optical and refraction-correction bathymetry (SfM correction); iv) comparing bathymetry detection for shallow natural multi-channel system and deeper artificial channels, and v) evaluating technical limitations related to the water level extraction as a factor for refraction corrections.

2 STUDY AREA

For bathymetry analyses, two different channel systems in Slovakia were selected. The first is a high-energy, multichannel, natural, and gravel-bed channel system of the Belá River (Fig. 1), and the second is an artificial, fine-sediment-dominant lowland canal, the Gabčíkovo–Topoľníky (Fig. 2).

Belá River

The Belá River is a high-energy river system in the northern part of Slovakia, with a catchment area of 244 km², located in the upper regions of the Western and High Tatra Mountains. According to the geomorphological division of Slovakia, the catchment belongs to two main geomorphological units: the Tatra Mountains and the Liptovská kotlina Basin (Lehotský et al., 2022; Mazúr and Lukniš, 1978). Sediments of the channel system reflect the general geological settings of the area, which are composed of pre-Mesozoic crystalline rocks (granitoid complex) and the Inner-Carpathian Paleogene sequences of the Zuberec and Huty formations (Gross et al., 1979). These sequences have a flyschoid character, characterised by alternating sandstone and claystone. These strata are overlaid by various Pleistocene glaciofluvial deposits (outwash) from the Tatras Mountains during the Pleistocene glaciation. The Holocene floodplain comprises boulders, gravel, and gravel-sandy fluvial deposits that are up to 2 m thick, with an average grain size diameter (D_{50}) of 126 mm (Kidová & Lehotský, 2012; Rusnák et al., 2020).

For the analyses, a 1.8 km long river reach in the downstream part of the catchment, near the village of Varišovo, was studied. A single- and multi-channel planform was selected for testing underwater bathymetry detection. The mean annual discharge for the Liptovský Hrádok gauging station, which is located 5 km downstream from the study area, is 6.8 $m^3.s^{-1}$ (Majerčáková et al., 2007). The channel in the upstream position is sinuous with gravel, present on both sides. In the downstream section, a river system is created with two arms at different vertical levels. The left channel, which serves as the feeding channel for a small hydropower plant and is artificially maintained, is situated at a higher elevation compared to the right channel.

Gabčíkovo–Topoľníky canal

The Gabčíkovo–Topoľníky canal is located on Rye Island in Slovakia, part of the Danube Lowland situated between the Danube River and the Little Danube River. Rye Island is characterised by a flat, lowland topography with a gentle inclination from northwest to southeast, averaging a slope of approximately 0.025%. Due to its flat terrain, favourable climatic conditions, and fertile soils, Rye Island ranks among the most productive agricultural regions in Slovakia. To protect this agriculturally valuable area from flooding, a canal network totalling nearly 1,000 km in length was constructed during the 18th century, originally intended to drain excess groundwater from agricultural fields. Over time, this network was adapted for irrigation purposes and to raise the groundwater table during periods of drought. Water levels and flow velocities in the region are primarily influenced by the Danube River, the Little Danube River, and the interconnected canals. However, flow rates in the canals are actively regulated, depending on seasonal variations, weather conditions, and agricultural demands (Bara et al., 2024).

Geologically, the area is underlain by Quaternary sediments, primarily comprising fluvial deposits of gravel with sand fractions, known as "Danubian gravels". These deposits reach a thickness of approximately 160 meters in the study area (Maglay et al., 2009). The sandy gravel formations create highly favourable conditions for groundwater accumulation and storage, forming the largest groundwater reservoir for Slovakia, and it is also the most significant in Eastern Europe. According to the Water Management Balance (WRI, 2005), the subsurface of Rye Island holds an estimated 10 billion cubic meters of potable water, equivalent to 18 $m^3.\ s^{-1}$ of available groundwater resources.

The specific study site is located in the central segment of the Gabčíkovo–Topoľníky Canal, between the villages of Vrakúň and Povoda. The canal spans a total

length of 28.7 river kilometres (rkm) and has an average width of 14 meters, ranging from 11 to 17 meters. For UAV-bathymetry, four separate sections of the canal, each with a length ranging from 200 m to 250 m, were selected. Two hydrological gauge stations are positioned along the canal: Gabčíkovo station at 25.7 rkm and Topoľníky station at 0.3 rkm. The elevation along the canal varies between 108.4 and 121.5 meters above sea level (m a.s.l.), sloping toward the Little Danube River.

Tab. 1. List of studies that used optical approach or SfM correction methods for reconstruction of underwater topography in fluvial geomorphology (approach for bathymetry detection - O -optical; SfM - refraction)

approach	analyses	country	river	platform	resolution	references
O	*water depth detection*	Finland	Tana and Pulmankijoki River	aerial RGB camera	50 cm/ 5 cm	Flener (2013)
		UK	Tay River	aerial multispectral camera	2 m	Bryant & Gilvear (1999)
		New Zealand	Waimakariri River	aerial RGB camera	7 cm	Westaway et al. (2003)
		New Zealand	Ahuriri River	UAV RGB camera	2 cm	Javernick et al. (2014)
		Finland	Pulmanki River	UAV RGB and aerial with a non-metric RGB camera	5 cm	Flener et al. (2013)
		France	Drôme River	UAV RGB camera	1 cm	Lejot et al. (2007)
		USA	Snake River and Soda Butte Creek	satellite (WorldView-2)	2 m	Legleiter & Overstreet (2012)
		USA	Salcha River	UAV RGB camera	10 cm	Legleiter & Kinzel (2021)
		USA	Laramie and Snake Rivers	aerial multispectral	1m	Legleiter (2013)
		USA	Snake River	aerial multispectral	50 cm	Legleiter (2016)
		UK	River Feshie	aerial RGB camera	25 cm	Brasington et al. (2003)
		New Zealand	Rees River	aerial with a non-metric RGB camera	20 cm	Williams et al. (2014)
	effect of morphology and reflectance relation to depth detection	USA	Brazos River	aerial RGB camera	20 cm	Fonstad & Marcus (2005)
		USA	Snake River	satellite (WorldView-2)	50 cm	Legleiter (2015)
		Canada	Lamar River	aerial multispectral	2.5 m	Legleiter & Roberts (2005)
		Canada	Kootenai River	aerial multispectral	50 cm	(Legleiter & Fosness (2019)
		Canada	Sainte-Marguerite River	aerial with a non-metric RGB camera	3 cm	Carbonneau et al. (2006)
	effect of field sampling point distribution	USA	Snake River	aerial multispectral	50 cm	Legleiter et al.(2018)
SfM	*depth detection from classic photogrammetry*	New Zealand	Ashburton River	aerial RGB camera	7.5 cm	Westaway et al. (2000, 2001)
	depth detection from Structure-from-Motion	USA	White River	UAV RGB camera	30 cm	Dietrich (2017)
		UK	River Arrow/ Coledale Beck	UAV RGB camera	9 cm	Woodget et al. (2015)
		UK	River Teme	UAV RGB camera	2 cm	Woodget et al. (2019)
		Slovakia	Belá River	UAV RGB camera	5 cm	Rusnák et al. (2024)
		Poland	Izera River	UAV RGB camera	1 cm	Witek et al. (2025)
	in-stream habitats classification and mapping	UK	River Arrow	UAV RGB camera	1cm	Woodget et al. (2016)
		Chile	San Pedro River	UAV RGB camera	1 cm (2 cm DEM)	Casado et al. (2015)
		UK	River Teme	UAV RGB camera	2 cm (2 cm DEM)	Woodget et al. (2017)
		Brazilia	Xingu River basin	UAV RGB camera	1.2 cm	Kalacska et al. (2018)
	bathymetry and hydraulic modelling	USA	South Fork Clearwater River	UAV RGB camera	no resolution	Timm et al. (2019)
		Canada	Elbow River	UAV RGB camera	5 cm	Tamminga et al. (2015)
SfM/O	*comparison of light refraction-correction (SfM) and optical bathymetry*	Finland	Pulmanki River	UAV RGB camera	3.4 cm	Kasvi et al. (2019)
		USA	Salmon River	UAV RGB camera	1.5 cm	Shintani & Fonstad (2017)
	sensor comparison	USA	Sacramento River	multispectral WorldView-3, Airborne hyperspectral CASI, UAV-based hyperspectral, Bathymetric LiDAR	1,36 m (WorlView-3); 50 cm (CASI); 18 cm (UAV) and 4 cm (LiDAR)	Legleiter & Harrison (2019)

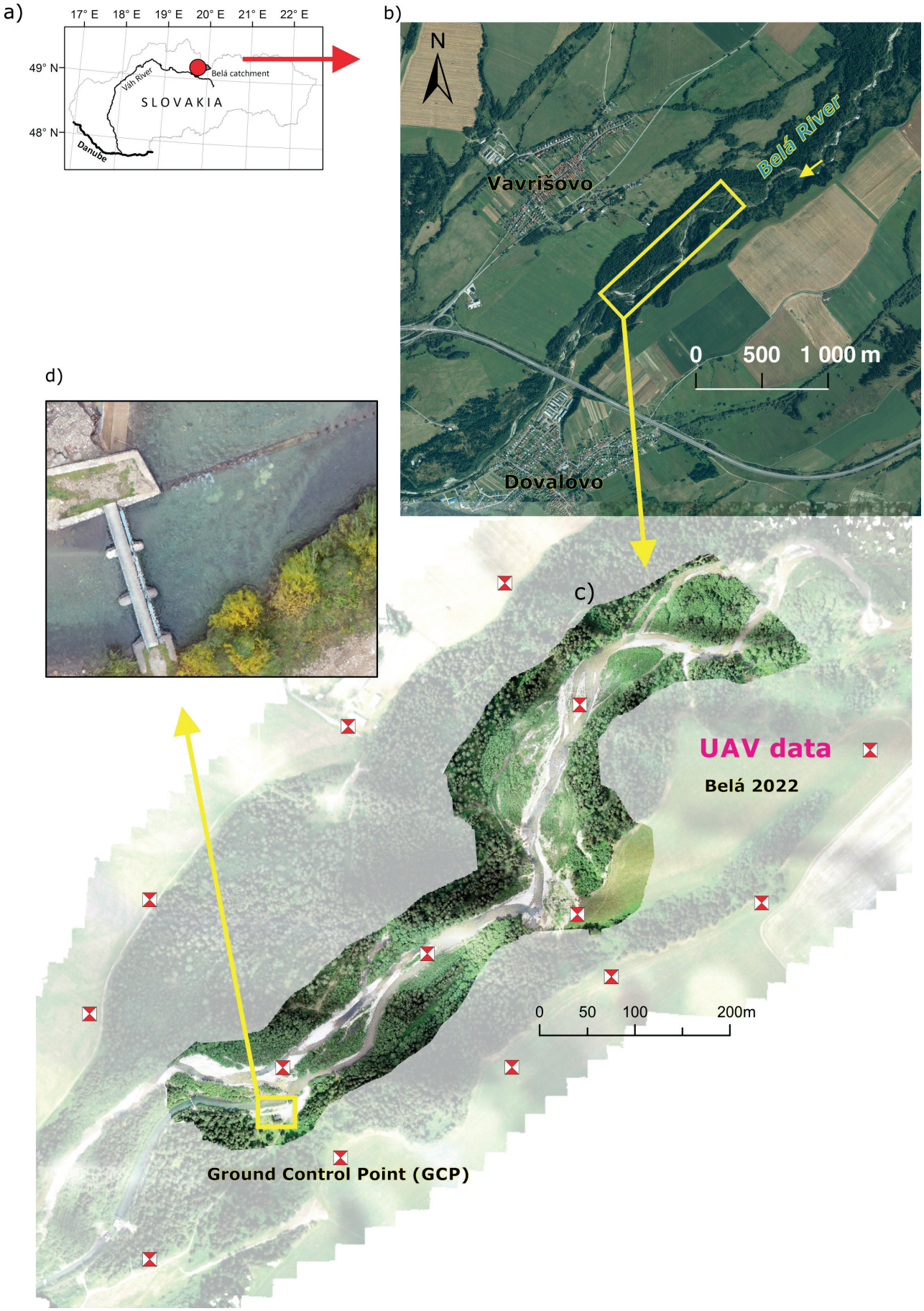


Fig. 1. General location of the Belá River in Slovakia (a). Position of the Belá River section selected for bathymetry extraction on orthophoto (b), detailed UAV orthophoto from 2022 (c), and detail of the channel bed topography in 2022 (d) and 2015 (e).

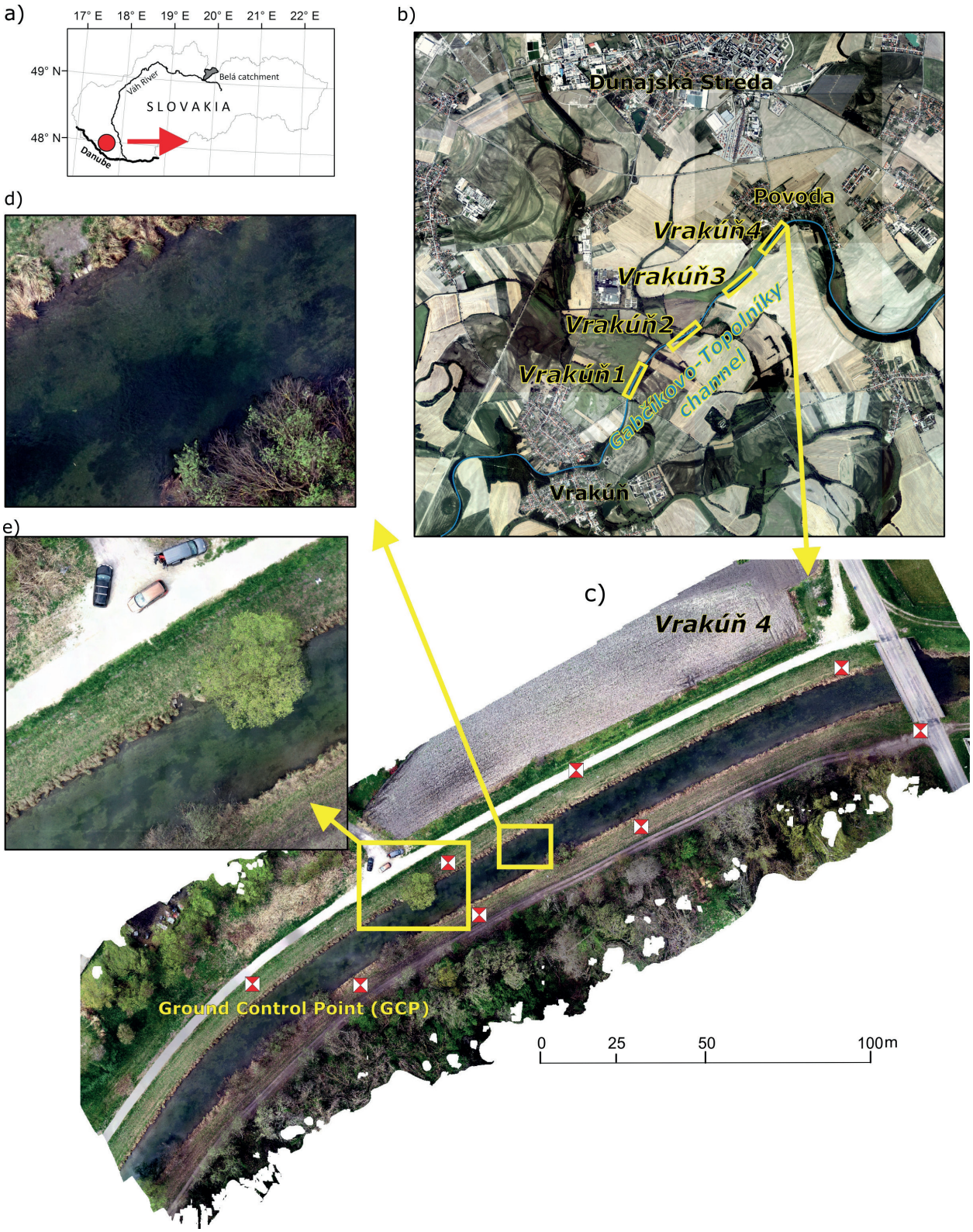


Fig. 2. General location of the Gabčíkovo-Topoľníky canal in Slovakia (a). Position of the studied sites on orthophoto (b), detailed UAV orthophoto of Vrakúň 4 study area from 2024 (c) and detail of the channel bed topography (d) and (c).

3 METHODS

UAV data processing

Bathymetry was analysed for seven UAV point clouds generated from RGB images in Agisoft Metashape software (Tab. 2). For the multichannel system of the Belá River, the temporal evolution of the bathymetry was compared for 2015 and 2022. For the Gabčíkovo–Topoľníky artificial canal, bathymetry was measured at four different spatial locations with varying water depths. UAV images were obtained using a HiSystem Hexakopter XL equipped with a Sony NEX 6 camera (Rusnák et al., 2018a, 2018b, 2024) and a DJI Phantom Pro4 with a sensor FC6310 (Rusnák et al., 2024). Spatial referencing was preserved with ground control points (GCP) measured using RTK-GNSS (RTK – Real-Time Kinematic, GNSS – Global Navigation Satellite System) devices with 1–2 cm position and vertical accuracy.

The distribution of GCP was selected to cover the entire scanned area, and it was evenly distributed for both the left and right banks. Distribution of the GCPs was selected to respect local conditions and vegetation cover, with a preference for bare surfaces and stable artificial objects, for optimal GCP replacement. During the flight, nadir and oblique imaging were combined to ensure higher geometric accuracy of the final point cloud and to remove the negative effects of the SfM algorithm and the non-metric camera (with the exception of Belá 2022). The final point cloud was exported in the S-JTSK national coordinates system (the unified trigonometric cadastral network; EPSG:5514), with a density of 150 - 400 points per m^2. In all campaigns, the point cloud was automatically classified to the ground using the Agisoft classification procedure. For the bank line vectorisation, a detailed orthophoto (2-5 cm) with elevation raster (DEM) was exported.

Generation of channel bathymetry

Refraction-correction bathymetry

The multi-view refraction-correction method was applied directly to the point cloud to remove the negative effects of light bending through a water-air interface. The SfM point cloud was modified using the pyBathySfM software (Dietrich, 2017; Woodget et al., 2018), which enabled the correction of water depth affected by refraction. The SfM-generated point cloud accurately captures the underwater channel bed topography in shallow and clear water; however, the elevation model is affected by errors related to refraction. The primary element for this approach is detecting the water surface from the point cloud, which determines the water-to-air interface and refraction point for light rays captured by the UAV sensor. The whole process of data processing can be divided into the following seven steps (Fig. 3): i) point cloud pre-processing; ii) bank line delimitation; iii) bank line elevation extraction; iv) bank line smoothing; v) water surface detection; vi) detection of uncorrected depth; vii) corrected depth calculation.

The point cloud was automatically classified as ground class using the Agisoft Metashape procedure to remove standing trees or artificial objects, and noise was reduced by the SOR filter (Statistical Outlier Removal) in CloudCompare. Bank lines were vectorised from detailed UAV orthophotos, and a hillshade was generated from a digital elevation model (DEM) from an SfM point cloud.

Bank elevation was extracted directly from the point cloud. For this procedure, the original point cloud was clipped using buffered bank lines (a 10 cm buffer), and the resulting clipped point cloud was manually checked and reclassified into two classes: noise and bank. For further processing, only the class bank was preserved and exported to multipoint with an elevation value. The bank line was transformed into points with a spacing of 10 cm, and based on the spatial join, the average elevation within a 50 cm distance from the clipped point cloud was extracted to the attribute table. A larger extracted distance (50 cm) than point spacing (10 cm) serves to smooth out possible uncertainties and errors in the delimitation of the bank line. Empty elevation values in the bank point were replaced with an interpolated raster from the clipped point cloud, created using linear binning methods with a 10 cm resolution.

The water surface was detected from the cross-section (XS_profile) line, which was automatically generated perpendicular to the channel centerline with a step of 1 m and a length of five meters longer than the channel width. To the endpoints of this XS_profiles, the median elevation from bank points (10 cm spacing) was extracted within a distance of 0.5 m from the XS_profile line. At the end, XS_profile lines were transformed into 3D lines and exported as a TIN surface. In the case of a multichannel planform, water surfaces were created separately for every channel and combined into a single water surface at the end.

Finally, in Cloud Compare, this TIN surface was converted to a mesh, and incorrect depths were calculated using a point-to-mesh distance method. For refraction correction, the pyBathySfM software, which includes a filtering function, was applied to incorporate refraction angles less than 35° off-nadir (Woodget et al., 2019).

Optical bathymetry

To estimate riverbed elevation from UAV imagery, a regression-based optical modelling approach was adopted to estimate riverbed bathymetry using high-resolution UAV orthophoto comprising passive optical RGB bands. The objective was to develop empirical relationships between image-derived radiance values and observed water depths recorded through in situ surveys. This approach was applied only for the Belá River study area.

To begin, UAV images were georeferenced, and spectral information was extracted at the exact geographic coordinates of the surveyed depth points. These values represent the total at-sensor radiance and are influenced by several factors beyond water depth, including the reflectance of the streambed, optical properties of the water column, and sunlight reflected off the water surface or scattered by the atmosphere (Legleiter, 2016). To minimise these external effects and emphasise the relationship between spectral response and depth, the input feature space was expanded by applying a series of mathematical transformations to the original RGB values. These included logarithmic scaling, normalised difference metrics, and ratio-based

Tab. 2. Parameters of UAV data processing in Agisoft Metashape software for different localities using in this study

code	date	No. of all images	No. of oblique images	sensor	No. GCP	GSD* [cm]	AGL** [m]	Z coord. RMSE*** [cm]	avg. channel depth**** [m]
bela_2015	22 Oct. 2015	1866	271	SONY NEX 6 (16–50 mm)	20	1.86	80, 50, 20	0.877	2.5 m
bela_2022	30 June 2022	2333	0	FC6310 (8.8mm)	14	2.65	112, 70	0.613	1.9 m
vrakun_1	25 March 2024	552	159	FC6310 (8.8mm)	8	1.02	75, 25, 15	1.069	2 m
vrakun_2	25 March 2024	481	274	FC6310 (8.8mm)	8	1.34	75, 35, 15	1.244	2.2 m
vrakun_3	25 March 2024	884	216	FC6310 (8.8mm)	8	0.97	75, 25, 15	0.525	1.1 m
vrakun_4	25 March 2024	156	35	FC6310 (8.8mm)	8	1.38	75, 25	0.899	1.4 m

*GSD – ground sampling distance; **AGL – above-ground level; *** RMSE – root mean square error of the height computed over all GCPs used for georeferencing, **** depth measured in the field

composites. These transformations help to linearise the exponential attenuation of light as described by Beer's Law, while also reducing the confounding influence of variable substrate reflectance and refraction effects (Lyzenga, 1978; Stumpf et al., 2003).

From the transformed dataset, all possible two-variable combinations were evaluated using three functional forms: linear, quadratic, and cross-quadratic models. The linear model represents a first-order relationship between spectral features and depth. The quadratic model includes squared terms of the input features to account for nonlinearity, while the cross-quadratic model extends this further by incorporating interaction terms between the two predictors. The general forms of these models are presented in Equations (1) to (3):

$$z = a_0 + a_1x_1 + a_2x_2 \quad (1)$$

$$z = a_0 + a_1x_1 + a_2x_2 + a_3(x_1)^2 + a_4(x_2)^2 \quad (2)$$

$$z = a_0 + a_1x_1 + a_2x_2 + a_3(x_1)^2 + a_4(x_2)^2 + a_5x_1x_2 \quad (3)$$

where z denotes water depth x_1 and x_2 are spectral features, and a_i are regression coefficients.

The dataset was split into training (70%) and validation (30%) subsets. Each model was fit on the training data and assessed using the Root Mean Square Error (RMSE) on the validation subset to quantify predictive performance. For each model type, the feature pair yielding the lowest RMSE was retained as optimal. These calibrated models were then applied to the full image dataset to generate continuous depth maps for the study area across two distinct temporal snapshots, facilitating comparison of riverbed morphology over time.

Validation datasets

An independent dataset of water depth was used for validation and modelling underwater bed-topography. For the Belá River, water depth was measured using an RTK-GNSS survey. The XY coordinates were obtained from GNSS with 1 - 2 cm positioning accuracy, and water depth was measured with a measuring tape mounted on a GNSS rod. For both campaigns, an overall total of 154 and 200 points was obtained for the Belá River in 2015 and 2022, respectively.

For the Gabčíkovo–Topoľníky channel, a commonly applied hydrological method based on the Doppler effect was used to measure streamflow, which enables simultaneous measurement of channel geometry and flow velocity within a defined profile. This method is implemented using a device known as an Acoustic Doppler Current Profiler (ADCP). An ADCP operates by emitting high-frequency ultrasonic pulses into a water column containing suspended particles; the movement of these particles causes a shift in the frequency of the reflected signals, which is used to calculate water velocity vectors (Mueller et al., 2013).

In this study, discharge and bathymetric measurements were conducted using the SonTek RiverSurveyor M9, a multi-frequency ADCP equipped with nine transducers: four operating at 1 MHz, four at 3 MHz, and a single vertical beam at 0.5 MHz dedicated to depth sounding. The use of multiple frequencies enhances the instrument's ability to resolve flow structures with higher spatial and temporal resolution, particularly in complex or shallow flow conditions. The device was deployed in moving-boat mode across multiple transects, capturing comprehensive three-dimensional flow and bathymetric data.

Post-processing of the raw ADCP data was performed using SonTek RiverSurveyorLive PC software, where parameters such as transducer depth, screening distance, magnetic declination, and GPS signal quality were validated to ensure data accuracy. The processed datasets were then exported in MATLAB format for further analysis using the Velocity Mapping Toolbox (VMT v4.09), a specialised software developed by the United States Geological Survey (USGS). VMT enables integration and spatial averaging of individual ADCP transects to generate a representative, smoothed cross-sectional profile of flow velocities and bathymetry. Finally, the ADCP cross-sectional profile point was converted to a point layer, and the average bathymetric depth within a 20 cm buffer was compared.

For the Belá River site, water depth was measured using an RTK-GNSS survey with centimetre-level precision. The depth was obtained by subtracting water level readings from measured bed elevations, with a total of 154 and 200 field points acquired in 2015 and 2022, respectively. This method provides direct, high-accuracy point measurements of both horizontal and vertical coordinates and thus represents a robust validation dataset for shallow-water conditions.

In contrast, the Gabčíkovo–Topoľníky canal (Vrakúň sites) was validated using an Acoustic Doppler Current Profiler (ADCP). Although it allows efficient profiling of deeper channels and provides dense cross-sectional data, its vertical precision is generally lower compared to RTK-GNSS surveys. ADCP-derived depths can be affected by beam geometry, signal scattering, water flow velocity, and GPS synchronisation accuracy. Therefore, while both reference datasets offer reliable control for bathymetric validation, their inherent differences in measurement principles and achievable accuracy must be acknowledged when interpreting the resulting error metrics.

To validate the model, a comparison between field-measured independent data and bathymetry topography was made, and the various metrics were calculated (Tab. 3), including the mean error (ME), the standard deviation error (SDE), the mean absolute error (MAE), and the root mean square error (RMSE). Spatial comparison of SfM-correction and optical bathymetry models was performed for the Belá River site, where both approaches were applied. From the optical approach, a linear model was selected, which exhibited the best results based on error metrics. Spatial harmonisation of datasets was secured by resampling of bathymetric rasters to a 10 cm resolution.

Tab. 3. Equation of validation metrics used for bathymetry dataset evaluation

error measure	equation
Mean error (ME)	$ME = \frac{\sum_i^n (x_{mod} - x_{obs})}{n}$
Standard deviation of error (SDE)	$SDE = \sqrt{\frac{\sum_i^n ((x_{mod} - x_{obs}) - ME)^2}{n - 1}}$
Mean absolute error (MAE)	$MAE = \frac{\sum_i^n \lvert x_{mod} - x_{obs} \rvert}{n}$
Root mean square error (RMSE)	$RMSE = \sqrt{\frac{\sum_i^n (x_{mod} - x_{obs})^2}{n}}$

Explanation: n – number of observations; x_{mod} – depth from model; x_{obs} – depth from validation dataset

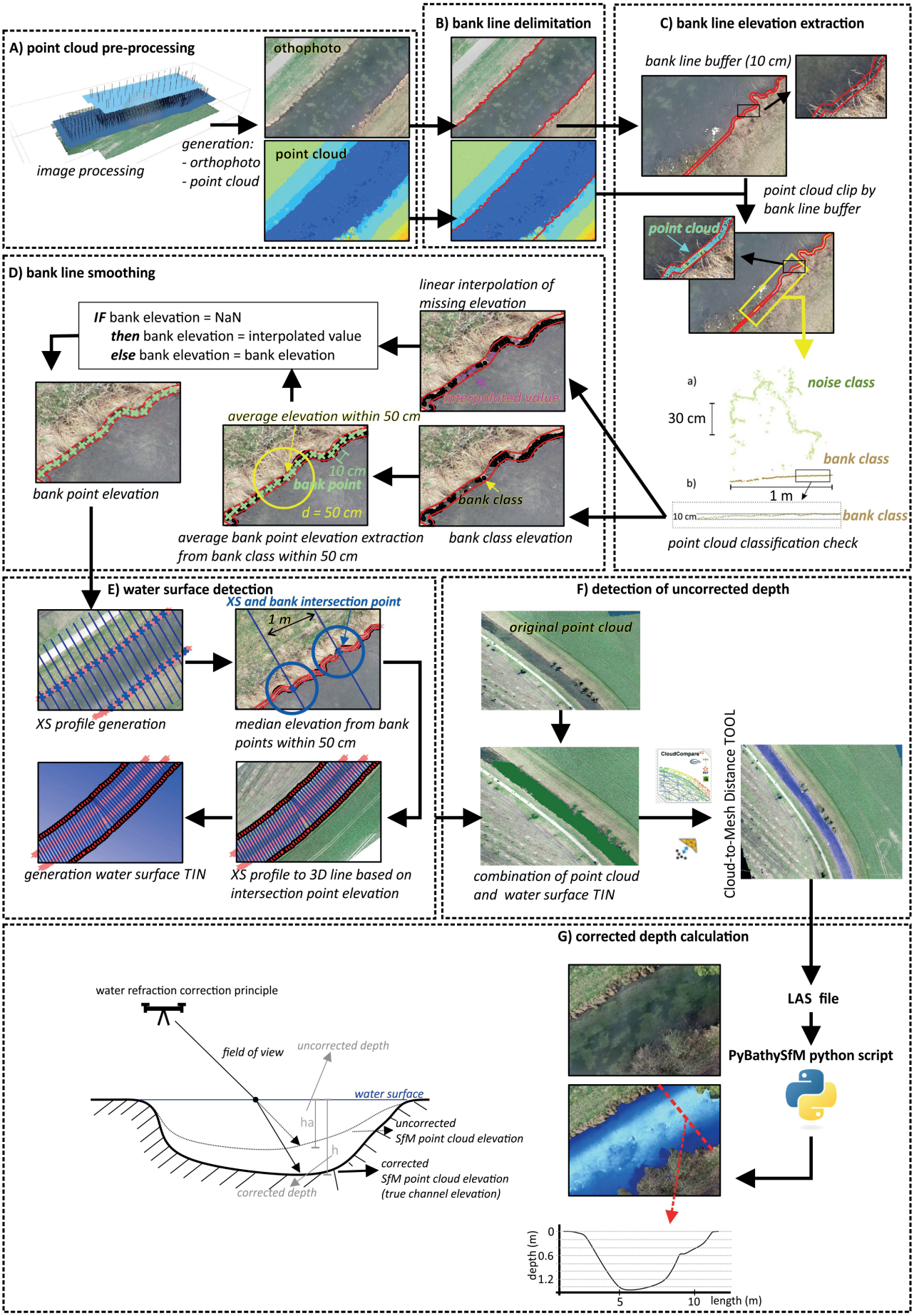


Fig. 3. Process of the multi-view refraction-correction method with individual steps: A) point cloud pre-processing; B) bank line delimitation; C) bank line elevation extraction; D) bank line smoothing; E) water surface detection; F) detection of uncorrected depth; and G) final corrected depth calculation with principal for refraction correction.

4 RESULTS

Refraction-correction bathymetry

A field dataset collected through a GNSS survey was used for validating the bathymetry model for the Belá River, and an ADCP was used for the Vrakúň site. Basic error metrics pointed to the accuracy of SfM-correction bathymetry with a mean error under 1 cm and RMSE up to 13 cm (Tab. 4) for GNSS survey validation. ADCP validation expresses higher error metrics up to 12 cm and ±30 cm for frequency distribution of the error that are mostly distributed within SDE (Fig. 4). Finally, a spatial continuous model of channel bed topography was created for all localities (Fig. 5). The result portrays very high reconstruction accuracy, which can capture small details and variations in bed elevation, as is represented by woody debris submerged under the water and a system of pools (deeper part of channel) and riffles (shallow water). For the Vrakuň site, it is impossible to reconstruct the channel bathymetry for the Vrakúň 1 and 2 sites for channel beds deeper than 2 m. Partially, the SfM point cloud detected the slopes of the underwear bank. However, the deepest sections are not captured in the SfM point cloud, and for that reason, it was subsequently impossible to perform a bathymetry correction.

Optical bathymetry

The performance of the bathymetric models derived from regression-based optical modelling was evaluated for each using standard statistical error metrics: the coefficient of determination (R^2), mean error (ME), standard deviation error (SDE), mean absolute error (MAE), and root mean square error (RMSE). For error calculation, independent testing datasets were used, with a total of 109 and 125 training points, and 47 and 56 testing points for the years 2015 and 2022, respectively. Table 5 summarises the results for all regression models tested across different years, including the selected input feature combinations, and the corresponding error statistics. A total of 153 feature combinations were generated by selecting pairs from the 18 derived spectral features (18C2). For each year, linear, quadratic, and cross-quadratic regression models were applied. The optimal model for each type was selected based on the lowest RMSE (Fig. 6, 7). The R^2 values reported in the table correspond to the correlation between the selected feature combination and observed depth, providing a measure of explanatory strength prior to regression fitting.

Comparison of refraction-correction and optical bathymetry

For the Belá River site, a direct spatial comparison was made between optical and SfM-correction bathymetry models for the 2015 and 2022 datasets. In general, elevation differences range from -2.9 m to 3.2 m, but the spatial distribution of elevation differences is mostly in a ± 25 cm range near zero values, with negligible frequency distribution errors more than 75 cm (Fig. 8). Higher elevation errors are connected with bifurcation reaches, which point to the problem of water surface detection for the SfM-correction approach. Prevalent positive differences indicated a larger depth value for the SfM algorithm, as compared to optical models. In reverse, negative values (blue) represent zones with overestimated depth values for the optical approach. Spatially, the blue sections are more related to the deeper pool sections of the river or zones in the tree shadow, as well as the positive differences in the riffle section of the river, and to the presence of bedrock outcropping.

Tab. 4. Result of bathymetric errors for refraction-correction methods between SfM bathymetry and field validation dataset (in meters)

model	type of bathymetry	n – number of validation points	error metrics (m)			
			ME	SDE	MAE	RMSE
Bela_2015	SfM-correction	154	-0.016	0.129	0.102	0.130
Bela_2022	SfM-correction	200	-0.005	0.112	0.086	0.111
vrakun_1	optical	13	0.166	0.296	0.257	0.330
vrakun_2	optical	8	0.117	0.114	0.152	0.158
vrakun_3	optical	81	-0.086	0.0856	0.104	0.121
vrakun_4	optical	42	-0.109	0.084	0.120	0.139

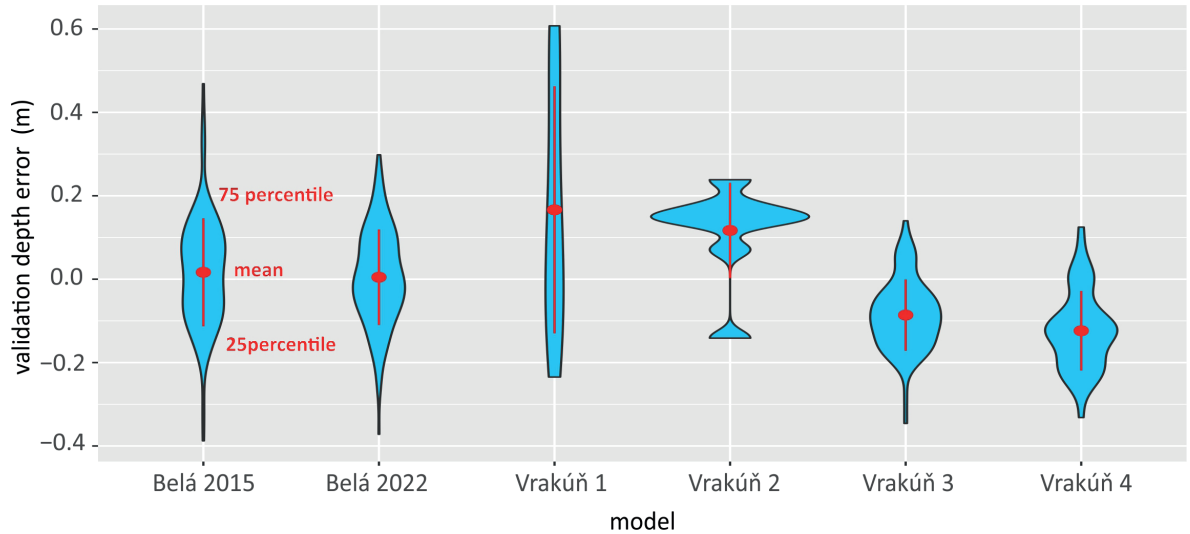


Fig. 4. Statistical distribution of depth error between validation datasets and corrected SfM-refraction bathymetric model.

Tab. 5. Result of bathymetric errors for regression-based optical modelling methods and field validation dataset (in meters).

Year	Model	Features	R^2	error metrics (m)			
				ME	SDE	MAE	RMSE
2015	Linear	Log(Blue),Log(Red/Green)	0.50	0.026	0.260	0.183	0.262
	Quadratic	Log(Blue), (Red/Green)	0.49	0.021	0.262	0.184	0.263
	Cross-Quadratic	Log(Blue), Log(Red/Green)	0.50	2.325	0.261	0.183	0.262
2022	Linear	Blue, Log(Red/Green)	0.47	0.007	0.155	0.121	0.155
	Quadratic	Log((Green-Blue)/ (Green+Blue)), (Red/Green)	0.53	0.012	0.146	0.115	0.147
	Cross-Quadratic	Blue, (Red -Green)/ (Red + Green	0.48	0.007	0.154	0.120	0.154

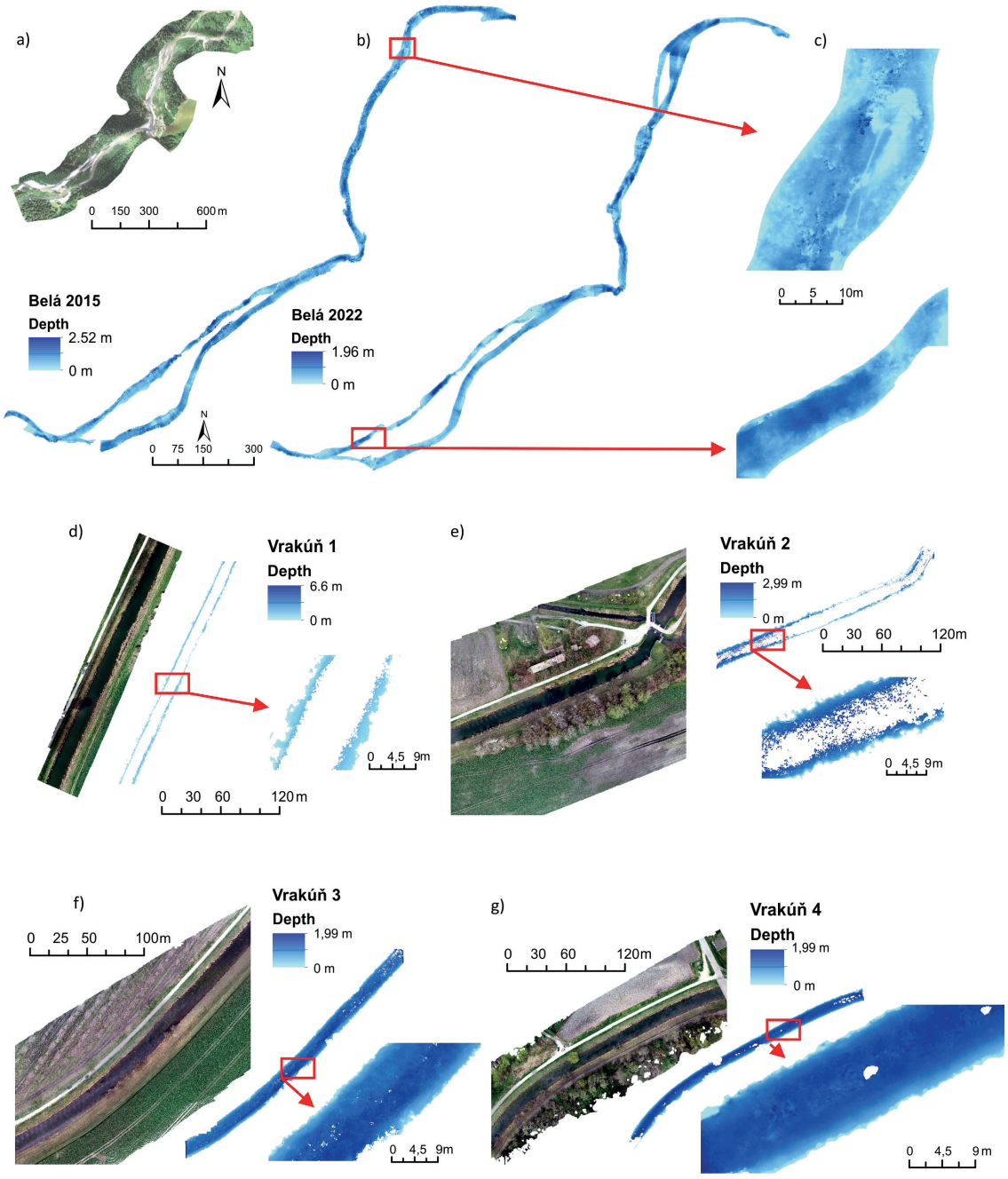


Fig. 5. Bathymetric model of channel depth for the Belá River (a) constructed from corrected depths from the UAV point cloud for 2015 and 2022 (b) with details on submerged trunk and deep pool section (c). Example of final bathymetric map with low reconstruction in deep channel for site Vrakúň 1 (d) or Vrakúň 2 (e), and completely continuous channel bathymetry for site Vrakúň 3 (f) and Vrakúň 4 (g).

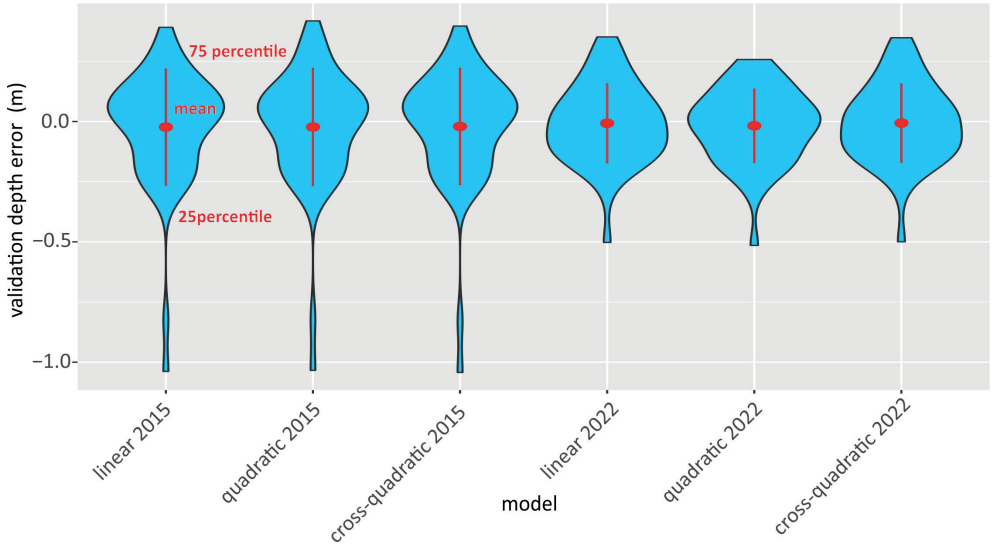


Fig. 6. Statistical distribution of depth error between validation datasets and optical bathymetric model for different feature combinations.

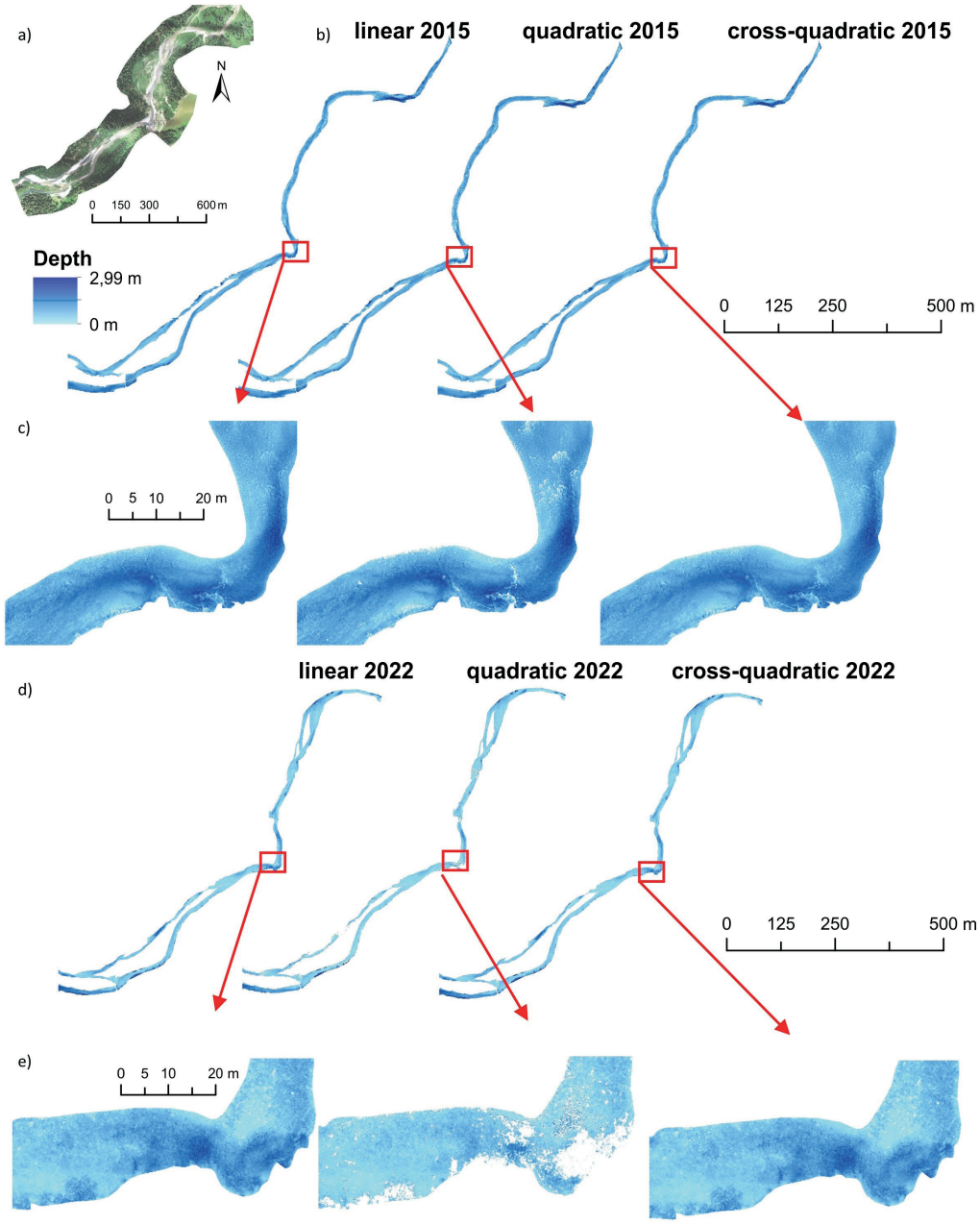


Fig. 7. Bathymetric model of channel depth for the Belá River (a) constructed based on an optical bathymetry approach from the UAV orthophoto from 2015 (b) with details on the deep pool section (c) and for 2022 (d) with details (e).

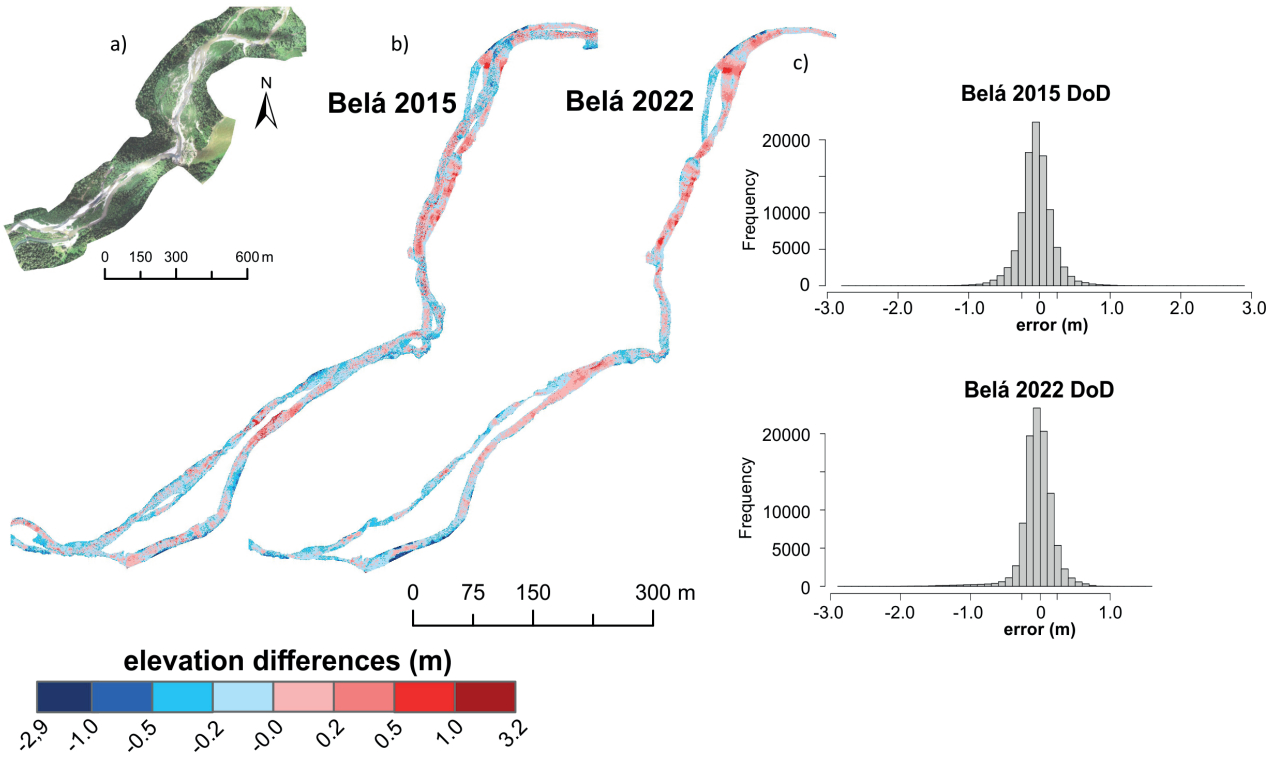


Fig. 8. Spatial comparison of elevation between SfM and optical bathymetry approach for the Belá River site (a), both datasets (c), and histogram of spatial errors distribution with 10 cm bin size (c).

5 DISCUSSION

Underwater bed-topography detection

The development of new technology enables the improvement of time effectiveness and accuracy of field data acquisition. UAV data and SfM can be used to detect high-resolution objects on the ground, as well as to reconstruct the underwater topography of the channel. Underwater elevation can be extracted directly from the point cloud using a refraction-correction approach, or modelled based on a statistical relationship between the spectral properties of pixels and field depth measurements. Moreover, water depth and underwater topography were reconstructed with an accuracy of ±15 cm, applying the optical-based approach and a 12 cm correction for refraction methods.

The results clearly indicated higher accuracy for the refraction-corrected SfM approach compared to optical bathymetry. However, this finding is partially influenced by differences in the precision of the reference datasets used for model validation. The Belá River bathymetry was validated using RTK-GNSS measurements, which provide centimetre-level accuracy in all XYZ directions, while the Gabčíkovo–Topoľníky canal was validated using ADCP sonar data. The ADCP survey achieves depth accuracy of several centimetres but lacks direct geodetic control, as its position depends on GPS synchronisation and boat trajectory. Consequently, part of the apparent accuracy difference between the two study areas may be attributed to the quality of the validation datasets rather than the performance of the UAV-derived models themselves.

Absolute error metrics (e.g., RMSE, MAE) between the Belá and Gabčíkovo–Topoľníky sites should therefore be interpreted as site-specific indicators, influenced by both environmental conditions (turbidity, flow velocity, depth) and the precision of the reference measurements. Future research should aim to integrate GNSS and ADCP observations into a unified validation framework to minimise cross-method biases and ensure consistent interpretation of UAV bathymetric accuracy across diverse hydraulic settings. The results can be affected by the varying precision of the validation dataset. The improved accuracy of the SfM-correction approach was validated using RTK-GNSS, achieving centimetre accuracy in all three directions (XYZ).

The refraction-correction method is less time-consuming and does not directly require field data measurement for depth retrieval (Dietrich, 2017; Kasvi et al., 2019). On the other hand, its final accuracy and precision are strongly related to the point cloud processing and overall georeferencing of the river channel model. Moreover, the process of detecting water levels or water surfaces is crucial for the proper application of corrections, which are spatially related to the light refraction boundary. Nevertheless, we can reach an RMSE of 12 cm for a multichannel natural river system. Similar results are also reached in other studies that used the SfM-correction approach, where depth error was estimated to ~10 cm (SDE) for the Pulmanki River in Finland (Kasvi et al. 2019), the meandering River Teme in the UK with RMSE 11.5 cm (Woodget et al. 2019), or 13 cm for the braided river Elbow (Tamminga et al., 2015). In all cases, the maximum river depth is 1.6, 1.43, or 1.5 m, respectively. Higher overall accuracy is achieved by Dietrich (2017), with an RMSE of 7.7 cm for White River or 6 cm from Arrow River (Woodget et al., 2015). In the study, Witek et al. (2025) tested 240 cases (2 sites × 5 profiles × 4 platforms × 3 resolutions × 2 repetitions), achieving an accuracy of 2.6 cm. They proved that the refraction-correction methods are robust for bathymetry detection, especially in terms of repeatability and reproducibility.

The optical approach using a deep-water model indicated a lower correlation (R^2 between 0.5 and 0.6) between field-measured depth and spectral reflectance. A similar correlation, ranging from 0.49 to 0.75, is also

noted by Carbonneau et al. (2006) and Westaway et al. (2003), who used high-resolution aerial images (5 and 7 cm). Legleiter (2013) and Bryant and Gilvear (1999) achieved correlation coefficients (R^2) of 0.68 and 0.67 using multispectral images. Higher correlation models were applied in the studies of Legleiter and Fosness (2019), utilising multispectral images for the meandering reach of the Kootenai River (R^2 = 0.83) and the Snake River (Legleiter, 2016), with coefficient R^2 values ranging from 0.83 to 0.92. Williams et al. (2014) utilised high-resolution aerial images to generate a bathymetric model, achieving a correlation coefficient of 0.81 for the braided Rees River in New Zealand. Moreover, the application of satellite images from WorldView-2 (with resolutions of 2 m and 50 cm) enables the mapping of bathymetry for large areas, achieving strong correlations of 0.82 and 0.67 (Legleiter & Overstreet, 2012; Legleiter, 2015).

UAVs are used for bathymetry detection of a braided river channel with 2 cm orthophoto resolution (Ahuriri River, New Zealand), achieving a correlation of 0.77 and a standard deviation error of 31 cm (Javernick et al., 2014). Lejot et al. (2007) applied a multilinear regression model (R^2 = 0.81) to the River Drôme, where orthophoto was captured using a Pixie UAV for a river with depths of up to 5 m and an error of 50 cm. UAV-images of meandering river systems with a resolution of 5 cm were used for the Pulmanki River (Finland) with R^2 = 0.75 and errors of 22.1 cm (Flener et al. 2013), and the the Salcha River (USA), achieving error metrics compared to echo-sounder measurement from 30 cm to 7.7 cm and R2 = 0.88 (Legleiter & Kinzel, 2021).

Based on the different studies that applied the optical and SfM bathymetry approach, overall accuracy is affected by the depth of the river (Fig. 9), with limitations of use in various studies that employed the optical and SfM bathymetry approach. Nevertheless, Legleiter et al. (2018) utilise optical bathymetry derived from multispectral imagery, validated by a multi-beam echo sounder, up to 8 meters. The maximum detectable depth of SfM is affected by water quality and water clarity, which enable the detection of structures for a multi-view matching algorithm on the channel bed (Dietrich, 2017).

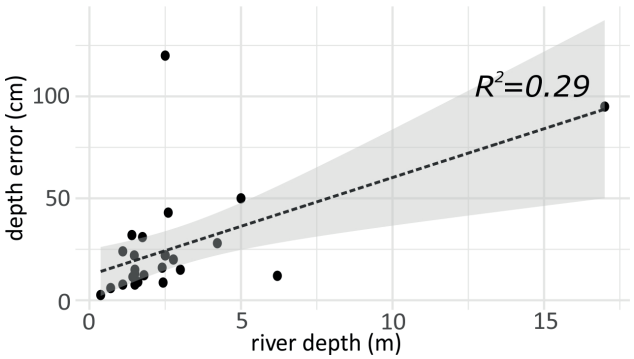


Fig. 9. Relationship between the depth error of bathymetry datasets generated based on optical and refraction-correction methods and the depth of rivers. The dataset was calculated based on the studies listed in Table 1.

Limits and errors of bathymetry processing

Clear advantages of remote sensing technology for evaluating and monitoring freshwater ecosystems include overcoming barriers that emerge with the application of technology, such as product accuracy, software, or programming personnel skills (Hestir et al., 2015). Underwater topography can be derived using spectral-depth models or by applying light refraction corrections in through-water photogrammetry and Structure-from-Motion (SfM) technologies. A common approach involves correlating spectral reflectance properties with empirically measured water depths. However, this method is limited by its inability to detect water depths exceeding a certain depth threshold. Moreover, this approach is sensitive to channel bed texture (substrate homogeneity), which can affect through-water radiance values. Higher or lower channel bed illumination can affect the final brightness values of DN numbers used in the deep-water radiance model (Flener, 2003). This can be affected by the amount of available sunlight during the time of imaging, or by the colour variability of the sediment bed composition (Legleiter & Roberts, 2004). A second important factor affecting final model accuracy is water turbidity, which has been extensively discussed in related technical literature (Kasvi et al., 2019). In both factors, this is evident in the Belá River, where the channel bed is covered by bright gravel and locally overlaid by grey and blue-violet claystone, resulting from vertical erosion and lateral migration inputs from the channel bank (Rusnák et al. 2020). When comparing the two-time horizons, clearer water with a sharp channel bed texture is visible in 2015, whereas the water in 2022 appears more turbid. Moreover, the mutual relationship between attenuation-based modelling can be affected by depth and band saturation lower than the maximum depth (Legleiter & Fosness, 2019). In the case of the Gabčíkovo–Topoľníky canal, the SfM bathymetry approach was unable to reconstruct the bottom of the canal if the channel depth exceeded more than 2 m. This limitation of the method stems from its primary principle, that the reconstructed surface must be visible in drone photographs. The algorithm for extracting tie points must be able to identify common points between individual images based on similar texture patterns. Significant depth, substrate type, or water turbidity affect light attenuation and bottom reflection. Without a visible channel bottom pattern, it is impossible to create an SfM model and subsequently reconstruct the depth of the channel.

Accurate mapping of submerged channel topography applying the SfM approach requires refraction correction, which typically relies on identifying the position and elevation of the water‘s edge (Woodget et al., 2015). Final accuracy is affected by georeferencing errors, point cloud noise, and the number of points detected underwater (Dietrich, 2017), as well as indirect atmospheric properties that influence sunlight penetration angle, water turbidity, and surface glittering. In general, model-associated errors are also associated with point cloud roughness (Dietrich, 2017; Woodget et al., 2019). Here, the result confirmed a higher error related to water surface detection for the Belá River, where the average gravel size is 126 mm (grain size sediment percentile D_{50}, Rusnák et al., 2020), which complicated the extraction of water surface elevation, and a higher smoothing window needs to be set. For the Gabčíkovo–Topoľníky artificial canal sites, water surface elevation cross-correlation errors are negligible. Furthermore, the Belá River is a steeper river system with multiple channels, which complicates water surface extrapolation (Rusnák et al., 2024). The final accuracy assessment is also sensitive to the accuracy of the independent validation dataset. Typically, RTK-GNSS measurements with a vertical accuracy of 2–4 cm, single-beam and multibeam echosounders, and ADCP are used. For sonars, the accuracy of channel topography datasets is lower, and they are unable to reproduce shallow water areas and small-scale topographic variability (Kasvi et al. 2019).

6 CONCLUSION

This study demonstrates that UAV-based photogrammetry provides a reliable and cost-efficient means of mapping shallow river bathymetry with sub-decimetre (0.1 m) accuracy. This study combined two complementary techniques, refraction-corrected Structure-from-Motion (SfM) photogrammetry and regression-based optical depth modelling, to evaluate their performance under contrasting hydromorphological and optical conditions.

The refraction-corrected SfM approach achieved the highest accuracy, with mean errors below 0.01 m and an RMSE of up to 0.13 m for the Belá River, as validated by RTK-GNSS measurements. For the Gabčíkovo–Topoľníky canal, RMSE values ranged from 0.12 m to 0.30 m when validated with ADCP sonar data. The optical bathymetry models, based solely on UAV RGB imagery, achieved RMSE values between 0.14 m and 0.23 m and coefficients of determination (R^2) ranging from 0.47 to 0.53, confirming acceptable performance in clear-water and shallow conditions.
Overall, the findings indicate that:

- SfM-based refraction correction delivers higher accuracy and is less dependent on water clarity,
- Optical regression models perform well when sufficient calibration data are available and environmental conditions are favourable,
- Both approaches capture fine-scale geomorphic features such as pools, riffles, and submerged wood that are often unresolved by conventional sonar-based methods.

UAV-derived bathymetry thus bridges the gap between ground surveys and large-scale remote sensing by enabling spatially continuous, repeatable, and high-resolution mapping of river channels. It provides valuable input for fluvial geomorphology, aquatic habitat assessment, and hydraulic modelling, particularly in environments where traditional sonar or LiDAR systems are limited.

It is essential to note that two distinct reference datasets were utilised for model validation: RTK-GNSS measurements for the Belá River (Vavrišovo site) and ADCP sonar measurements for the Gabčíkovo–Topoľníky canal (Vrakúň sites). These datasets differ in measurement principle, spatial density, and achievable accuracy. GNSS surveys provide direct point-based depth data with vertical precision better than 0.02 m, whereas ADCP sonar is affected by beam geometry, flow velocity, and GPS synchronisation, resulting in several-centimetre uncertainty. Consequently, the reported RMSE values between the two sites are not directly comparable, as part of the observed discrepancy may originate from the accuracy of the reference datasets rather than from the UAV-derived models themselves. Future research should therefore aim to establish a consistent validation framework, ideally combining RTK-GNSS control points with synchronised sonar transects to minimise cross-method bias and improve the comparability of UAV bathymetric assessments across different fluvial environments.

Despite its overall potential, UAV bathymetry still faces technical challenges. The optical depth inversion is highly dependent on water clarity, substrate reflectance, and illumination, while the robustness of refraction-corrected SfM relies on accurate water-surface detection and stable georeferencing. Addressing these limitations will require the development of enhanced algorithms for automated water-surface extraction, improved radiometric calibration, and the integration of multi- or hyperspectral sensors. Such developments will strengthen the role of UAV-based topo-bathymetry as a precise and repeatable tool for monitoring channel morphology and geomorphic change in complex river systems.

Overall, UAV-derived bathymetry represents a transformative step toward integrating high-resolution topographic and hydraulic data for process-based fluvial research. Furthermore, it presents a critical link between field-based topographic surveys and large-scale remote sensing, enabling cost-effective, spatially continuous, and temporally repeatable mapping of channel morphology (Sládek & Rusnák, 2013, 2017). Such developments will enhance our ability to monitor and model geomorphic change, providing new insights into the spatial and temporal evolution of river systems. Despite its advantages, several limitations arise from the combination of methods and tools (Buša et al., 2020; Dušeková et al. 2024; Lehotský et al. 2024; Kovanič et al. 2025; Pukanská et al. 2024; Šašák et al., 2019). The operational application of remote sensing techniques enlarges data computing capacity, storage, and technological knowledge. In practice, application in field settings, including the validation of methods and the identification of their detection limitations, requires specific skills (Rusnák et al. 2022). Despite its potential, SfM is frequently adopted by users lacking formal training or without appropriate methodological adaptation. This can lead to unaddressed systematic errors, increased uncertainty, and insufficient use of independent verification measurements (Eltner et al., 2021; James & Robson, 2014; Kršák et al. 2016; Sanz-Ablanedo et al., 2020).

Acknowledgements:

The study was supported by the Science Grant Agency (VEGA) of the Ministry of Education, Science, Research and Sport of the Slovak Republic and the Slovak Academy of Sciences [Grant No. 02/0016/24 and No. 02/0028/23] and by the Slovak Research and Development Agency under Contract No. APVV-23-0265. The authors are grateful to the Government of the Slovak Republic, which provided a mobility grant from the National Scholarship Programme of the Slovak Republic (Rohit Sharma). The authors would like to thank the reviewers for taking the time and effort necessary to review the manuscript. The authors sincerely appreciate all the valuable comments and suggestions that helped us improve the quality of the manuscript.

REFERENCES

Bara, M.K., Dulovičová, R., Velísková, Y. & Farkas, C. (2024). Impacts of riverbed aggradation on groundwater regime in a lowland area. Journal of Hydrology and Hydromechanics, 72(2),185–198. https://doi.org/10.2478/johh-2024-0002

Brasington, J., Langham, J., & Rumsby, B. (2003). Methodological sensitivity of morphometric estimates of coarse fluvial sediment transport. Geomorphology, 53(3–4), 299–316. https://doi.org/10.1016/S0169-555X(02)00320-3

Buša, J., Rusnák, M., Kušnirák, D., Greif, V., Bednarik, M., Putiška, R., Dostál, I., Sládek, J., & Rusnáková, D. (2020). Urban landslide monitoring by combined use of multiple methodologies - a case study on Sv. Anton town, Slovakia. Physical Geography, 41(2), 169–194. https://doi.org/10.1080/02723646.2019.1630232

Bryant, R. G., & Gilvear, D. J. (1999). Quantifying

geomorphic and riparian land cover changes either side of a large flood event using airborne remote sensing: River Tay, Scotland. Geomorphology, 29(3–4), 307–321. https://doi.org/10.1016/S0169-555X(99)00023-9

Carbonneau, P. E., Lane, S. N., & Bergeron, N. (2006). Feature based image processing methods applied to bathymetric measurements from airborne remote sensing in fluvial environments. Earth Surface Processes and Landforms, 31(11), 1413–1423. https://doi.org/10.1002/esp.1341

Casado, M., Gonzalez, R., Kriechbaumer, T., & Veal, A. (2015). Automated Identification of River Hydromorphological Features Using UAV High Resolution Aerial Imagery. Sensors, 15(11), 27969–27989. https://doi.org/10.3390/s151127969

Dietrich, J. T. (2017). Bathymetric Structure-from-Motion: extracting shallow stream bathymetry from multi-view stereo photogrammetry. Earth Surface Processes and Landforms, 42(2), 355–364. https://doi.org/10.1002/esp.4060

Dušeková, L., Herich, P., Pukanská, K., Bartoš, K., Kseňak, Ľ., Šveda, J., & Fehér, J. (2024). Comparison of Non-Contact Measurement Technologies Applied on the Underground Glacier—The Choice for Long-Term Monitoring of Ice Changes in Dobšiná Ice Cave. Remote Sensing, 16(20). https://doi.org/10.3390/rs16203870

Eltner, A., Bertalan, L., Grundmann, J., Perks, M. T., & Lotsari, E. (2021). Hydromorphological mapping of river reaches using videos captured with UAS. Earth Surface Processes and Landforms. 46(14),2773–2787.https://doi.org/10.1002/esp.5205

Flener, C. (2013). Estimating deep water radiance in shallow water: Adapting optical bathymetry modelling to shallow river environments. Boreal Environment Research, 18(6), 488–502.

Flener, C., Vaaja, M., Jaakkola, A., Krooks, A., Kaartinen, H., Kukko, A., Kasvi, E., Hyyppä, H., Hyyppä, J., & Alho, P. (2013). Seamless Mapping of River Channels at High Resolution Using Mobile LiDAR and UAV-Photography. Remote Sensing, 5(12), 6382–6407. https://doi.org/10.3390/rs5126382

Fonstad, M. A., & Marcus, W. A. (2005). Remote sensing of stream depths with hydraulically assisted bathymetry (HAB) models. Geomorphology, 72(1–4), 320–339. https://doi.org/10.1016/j.geomorph.2005.06.005

Gross, P., Vaškovský, I., & Halouzka, R. (1979). Geologická mapa Liptovskej kotliny [Geological map of Liptovská kotlina basin]. GÚDŠ, Bratislava.

Hestir, E. L., Brando, V. E., Bresciani, M., Giardino, C., Matta, E., Villa, P., & Dekker, A. G. (2015). Measuring freshwater aquatic ecosystems: The need for a hyperspectral global mapping satellite mission. Remote Sensing of Environment, 167, 181–195. https://doi.org/10.1016/j.rse.2015.05.023

Javernick, L., Brasington, J., & Caruso, B. (2014). Modeling the topography of shallow braided rivers using Structure-from-Motion photogrammetry. Geomorphology, 213, 166–182. https://doi.org/10.1016/j.geomorph.2014.01.006

James, M. R., & Robson, S. (2014). Mitigating systematic error in topographic models derived from UAV and ground-based image networks. Earth Surface Processes and Landforms, 39(10), 1413–1420. https://doi.org/10.1002/esp.3609

Kalacska, M., Lucanus, O., Sousa, L., Vieira, T., & Arroyo-Mora, J. (2018). Freshwater Fish Habitat Complexity Mapping Using Above and Underwater Structure-From-Motion Photogrammetry. Remote Sensing, 10(12), 1912. https://doi.org/10.3390/rs10121912

Kasvi, E., Salmela, J., Lotsari, E., Kumpula, T., & Lane, S. N. (2019). Comparison of remote sensing based approaches for mapping bathymetry of shallow, clear water rivers. Geomorphology, 333, 180–197. https://doi.org/10.1016/j.geomorph.2019.02.017

Kidová, A., & Lehotský, M. (2012). Časovo-priestorová variabilita morfológie divočiaceho a migrujúceho vodného toku Belá. Geografický Časopis, 64(4), 311–333.

Kovanič, Ľ., Peťovský, P., Topitzer, B., Blišťan, P., & Tokarčík, O. (2025). Analysis of the Qualitative Parameters of Mobile Laser Scanning for the Creation of Cartographic Works and 3D Models for Digital Twins of Urban Areas. Applied Sciences, 15(4), 2073. https://doi.org/10.3390/app15042073

Kršák, B., Blišťan, P., Pauliková, A., Puškárová, P., Kovanič, Ľ., Palková, J., & Zelizňaková, V. (2016). Use of low-cost UAV photogrammetry to analyze the accuracy of a digital elevation model in a case study. Measurement, 91, 276–287. https://doi.org/10.1016/j.measurement.2016.05.028

Lague, D., & Feldmann, B. (2020). Topo-bathymetric airborne LiDAR for fluvial-geomorphology analysis. Developments in Earth Surface Processes, 23, 25–54. https://doi.org/10.1016/B978-0-444-64177-9.00002-3

Legleiter, C., & Fosness, R. (2019). Defining the Limits of Spectrally Based Bathymetric Mapping on a Large River. Remote Sensing, 11(6), 665. https://doi.org/10.3390/rs11060665

Legleiter, C. J. (2013). Mapping river depth from publicly available aerial images. River Research and Applications, 29(6), 760–780. https://doi.org/10.1002/rra.2560

Legleiter, C. J. (2015). Calibrating remotely sensed river bathymetry in the absence of field measurements: Flow REsistance Equation-Based Imaging of River Depths (FREEBIRD). Water Resources Research, 51(4), 2865–2884. https://doi.org/10.1002/2014WR016624

Legleiter, C. J. (2016). Inferring river bathymetry via Image-to-Depth Quantile Transformation (IDQT). Water Resources Research, 52(5), 3722–3741. https://doi.org/10.1002/2016WR018730

Legleiter, C. J. (2021). The optical river bathymetry toolkit. River Research and Applications, 37(4), 555–568. https://doi.org/10.1002/RRA.3773

Legleiter, C. J., & Harrison, L. R. (2019). Remote Sensing of River Bathymetry: Evaluating a Range of Sensors, Platforms, and Algorithms on the Upper Sacramento River, California, USA. Water Resources Research, 55(3), 2142–2169. https://doi.org/10.1029/2018WR023586

Legleiter, C. J., & Kinzel, P. J. (2021). Improving Remotely Sensed River Bathymetry by Image-Averaging. Water Resources Research, 57(3), e2020WR028795. https://doi.org/10.1029/2020WR028795

Legleiter, C. J., & Overstreet, B. T. (2012). Mapping gravel bed river bathymetry from space. Journal of Geophysical Research: Earth Surface, 117(F04024). https://doi.org/10.1029/2012JF002539

Legleiter, C. J., & Roberts, D. A. (2005). Effects of channel morphology and sensor spatial resolution on image-derived depth estimates. Remote Sensing of Environment, 95(2), 231–247. https://doi.org/10.1016/j.rse.2004.12.013

Legleiter, C., Overstreet, B., & Kinzel, P. (2018).

Sampling Strategies to Improve Passive Optical Remote Sensing of River Bathymetry. Remote Sensing, 10(6), 935. https://doi.org/10.3390/rs10060935

Lehotský, M., Rusnák, M., & Novotný, J. (2022). Short History of Geomorphological Research and Geomorphological Division of Slovakia (pp. 1–5). https://doi.org/10.1007/978-3-030-89293-7_1

Lehotský, M., Horáčková, Š., Rusnák, M., Štefanička, T., & Kleň, J. (2024). Morphologic Adjustment of a River Reach with Groynes to Channel Bypassing. Pure and Applied Geophysics, 181, 977–1001. https://doi.org/10.1007/s00024-024-03433-z

Lejot, J., Delacourt, C., Piégay, H., Fournier, T., Trémélo, M.-L., & Allemand, P. (2007). Very high spatial resolution imagery for channel bathymetry and topography from an unmanned mapping controlled platform. Earth Surface Processes and Landforms, 32(11), 1705–1725. https://doi.org/10.1002/esp.1595

Lurton, X. (2010). An Introduction to Underwater Acoustics: Principles and Applications. Springer Berlin, Heidelberg. https://link.springer.com/book/9783540784807

Lyzenga, D. R. (1978). Passive remote sensing techniques for mapping water depth and bottom features. Applied Optics, 17(3), 379–383. https://doi.org/10.1364/AO.17.000379

Maglay, J. et al. 2009. Quaternary geological map of Slovakia - Map of Quaternary cover thickness, M 1: 500000. Slovak Geological Institute of Dionyz Stur, Bratislava.

Majerčáková, O., Škoda, P., & Danáčová, Z. (2007). Vývoj vybraných hydrologických a zrážkových charakteristík za obdobia 1961–2000 a 2001–2006 v oblasti Vysokých Tatier [The development of selected hydrological and precipitation characteristics of 1961-2000 and 2001-2006 periods in High Tatras region]. Meteorologický Časopis, 10(4), 205–210.

Mazúr, E., & Lukniš, M. (1978). Regionálne Geomorfologické Členenie SSR [Regional geomorphic division of Slovakia]. Geografický Časopis, 30(1), 101–125.

Mueller, D. S., Wagner, C. R., & Rehmann, C. R. (2013). Measuring discharge with acoustic Doppler current profilers from a moving boat (Techniques and Methods 3–A22). U.S. Geological Survey. https://doi.org/10.3133/tm3A22

Pukanská, K., Bartoš, K., Gašinec, J., Pašteka, R., Zahorec, P., Papčo, J., Bella, P., Andrássy, E., Dušeková, L., Bobíková, D., & Kseňak, Ľ. (2024). Methodological approaches to survey complex ice cave environments - the case of Dobšiná (Slovakia). Frontiers in Environmental Science, 12. https://doi.org/10.3389/fenvs.2024.1484169

Rusnák, M., Goga, T., Michaleje, L., Michalková, M. Š., Máčka, Z., Bertalan, L., & Kidová, A. (2022). Remote Sensing of Riparian Ecosystems. Remote Sensing, 14(11), 2645. https://doi.org/10.3390/rs14112645

Rusnák, M., Kaňuk, J., Kidová, A., Lehotský, M., Piégay, H., Sládek, J., & Michaleje, L. (2024). Inferring channel incision in gravel-bed rivers: Integrating LiDAR data, historical aerial photographs and drone-based SfM topo-bathymetry. Earth Surface Processes and Landforms, 49(8), 2475–2497. https://doi.org/10.1002/esp.5840

Rusnák, M., Kaňuk, J., Kidová, A., Šašak, J., Lehotský, M., Pöppl, R., & Šupinský, J. (2020). Channel and cut-bluff failure connectivity in a river system: Case study of the braided-wandering Belá River, Western Carpathians, Slovakia. Science of The Total Environment, 733, 139409. https://doi.org/10.1016/j.scitotenv.2020.139409

Rusnák, M., Kidová, A., Lehotský, M., & Sládek, J. (2022). Fluvial Imprints in Flysh Valley Bottoms—Topľa and Ondava Valleys (M. Lehotský & M. Boltižiar, Eds.; pp. 307–321). Springer International Publishing. https://doi.org/10.1007/978-3-030-89293-7_16

Rusnák, M., Lehotský, M., Kidová, A., & Sládek, J. (2018). Metamorfózy korýt štrkonosných vodných tokov (Issue 2). Geomorphologia Slovaca et Bohemica.

Rusnák, M., Sládek, J., & Kidová, A. (2018). Využitie UAV technológie pre klasifikáciu a mapovanie krajiny vo fluviálnej geomorfológii. Geografický Časopis - Geographical Journal, 70(2), 141–160. https://doi.org/10.31577/geogrcas.2018.70.2.08

Rusnák, M., Sládek, J., Kidová, A., & Lehotský, M. (2018). Template for high-resolution river landscape mapping using UAV technology. Measurement, 115, 139–151. https://doi.org/10.1016/j.measurement.2017.10.023

Sanz-Ablanedo, E., Chandler, J. H., Ballesteros-Pérez, P., & Rodríguez-Pérez, J. R. (2020). Reducing systematic dome errors in digital elevation models through better UAV flight design. Earth Surface Processes and Landforms, 45(9), 2134–2147. https://doi.org/10.1002/esp.4871

Šašak, J., Gallay, M., Kaňuk, J., Hofierka, J., & Minár, J. (2019). Combined Use of Terrestrial Laser Scanning and UAV Photogrammetry in Mapping Alpine Terrain. Remote Sensing, 11(18), 2154. https://doi.org/10.3390/rs11182154

Shintani, C., & Fonstad, M. A. (2017). Comparing remote-sensing techniques collecting bathymetric data from a gravel-bed river. International Journal of Remote Sensing, 38(8–10), 2883–2902. https://doi.org/10.1080/01431161.2017.1280636

Sládek, J., & Rusnák, M. (2013). Nizkonákladove mikro-UAV techológie v geografii (nová metóda zberu priestorových dát). Geograficky Časopis, 65(3), 269–285.

Sládek, J., & Rusnák, M. (2017). Bezpilotné systémy vo fyzickej geografii. Biologie. Chemie. Zeměpis, 26(4), 2–17. https://doi.org/10.14712/25337556.2017.4.1

Smith, W. H. F., & Sandwell, D. T. (1997). Global sea floor topography from satellite altimetry and ship depth soundings. Science, 277(5334), 1956–1962. https://doi.org/10.1126/SCIENCE.277.5334.1956/ASSET/FBFA5CB2-0680-4A97-B98D-A5648B80563E/ASSETS/GRAPHIC/SE3875739005.JPEG

Stumpf, R. P., Holderied, K., & Sinclair, M. (2003). Determination of water depth with high-resolution satellite imagery over variable bottom types. Limnology and Oceanography, 48(1,2), 547–556. https://doi.org/10.4319/lo.2003.48.1_part_2.0547

Tamminga, A., Hugenholtz, C., Eaton, B., & Lapointe, M. (2015). Hyperspatial Remote Sensing of Channel Reach Morphology and Hydraulic Fish Habitat Using an Unmanned Aerial Vehicle (UAV): A First Assessment in the Context of River Research and Management. River Research and Applications, 31(3), 379–391. https://doi.org/10.1002/rra.2743

Westaway, R. M., Lane, S. N., & Hicks, D. M. (2000). The development of an automated correction procedure for digital photogrammetry for the study of wide, shallow, gravel-bed rivers. Earth Surface Processes and Landforms, 25(2), 209–

226. https://doi.org/10.1002/(SICI)1096-9837(200002)25:2<209::AID-ESP84>3.0.CO;2-Z

Westaway, R. M., Lane, S. N., & Hicks, D. M. (2001). Remote Sensing of Clear-Water, Shallow, Gravel-Bed Rivers Using Digital Photogrammetry. Photogrammetric Engineering & Remote Sensing, 67(11), 1271–1281.

Westaway, R. M., Lane, S. N., & Hicks, D. M. (2003). Remote survey of large-scale braided, gravel-bed rivers using digital photogrammetry and image analysis. International Journal of Remote Sensing, 24(4), 795–815. https://doi.org/10.1080/01431160110113070

Williams, R. D., Brasington, J., Vericat, D., & Hicks, D. M. (2014). Hyperscale terrain modelling of braided rivers: fusing mobile terrestrial laser scanning and optical bathymetric mapping. Earth Surface Processes and Landforms, 39(2), 167–183. https://doi.org/10.1002/esp.3437

Witek, M., Walusiak, G., Halicki, M., Remisz, J., Borowicz, D., Parzóch, K., Kasprzak, Ł., Langhammer, J., Gallay, M., Miřijovský, J., Šašak, J., Kaňuk, J., Lendzioch, T., Minařík, R., Popelka, S., & Niedzielski, T. (2025). Reconstructing bed topography of a shallow river from close-range aerial imagery: Multi-UAV experimental campaign in the Izera river (SW Poland/N Czechia). Geomorphology, 471, 109544. https://doi.org/10.1016/j.geomorph.2024.109544

Woodget, A. S., & Austrums, R. (2017). Subaerial gravel size measurement using topographic data derived from a UAV-SfM approach. Earth Surface Processes and Landforms, 42(9), 1434–1443. https://doi.org/10.1002/esp.4139

Woodget, A. S., Austrums, R., Maddock, I. P., & Habit, E. (2017). Drones and digital photogrammetry: from classifications to continuums for monitoring river habitat and hydromorphology. Wiley Interdisciplinary Reviews: Water, 4(4), e1222. https://doi.org/10.1002/wat2.1222

Woodget, A. S., Carbonneau, P. E., Visser, F., & Maddock, I. P. (2015). Quantifying submerged fluvial topography using hyperspatial resolution UAS imagery and structure from motion photogrammetry. Earth Surface Processes and Landforms, 40(1), 47–64. https://doi.org/10.1002/esp.3613

Woodget, A. S., Dietrich, J. T., & Wilson, R. T. (2019). Quantifying Below-Water Fluvial Geomorphic Change: The Implications of Refraction Correction, Water Surface Elevations, and Spatially Variable Error. Remote Sensing, 11(20), 2415. https://doi.org/10.3390/rs11202415

Woodget, A. S., Fyffe, C., & Carbonneau, P. E. (2018). From manned to unmanned aircraft: Adapting airborne particle size mapping methodologies to the characteristics of sUAS and SfM. Earth Surface Processes and Landforms, 43(4), 857–870. https://doi.org/10.1002/ESP.4285

Woodget, A. S., Visser, F., Maddock, I. P., & Carbonneau, P. E. (2016). The Accuracy and Reliability of Traditional Surface Flow Type Mapping: Is it Time for a New Method of Characterizing Physical River Habitat? River Research and Applications, 32(9), 1902–1914. https://doi.org/10.1002/rra.3047

Yunus, A. P., Dou, J., Song, X., & Avtar, R. (2019). Improved Bathymetric Mapping of Coastal and Lake Environments Using Sentinel-2 and Landsat-8 Images. Sensors, 19(12), 2788. https://doi.org/10.3390/S19122788

Article first received: 9 June 2025
Article accepted: 20 November 2025